Ocular Oncology and Pathology

Research Article

Ocul Oncol Pathol 2021;7:330–339
DOI: 10.1159/000515142

Received: August 26, 2020
Accepted: February 8, 2021
Published online: June 2, 2021

Optical Coherence Tomography Angiography Microvascular Variations in Pre- and Posttreatment of Retinoblastoma Tumors

Juan P. Fernandez Asghar A. Haider Lejla Vajzovic Arathi Ponugoti
Michael P. Kelly Miguel A. Materin

Department of Ophthalmology, Duke University, Durham, NC, USA

Keywords
Optical coherence tomography angiography · Retinoblastoma · Microvasculature · Chemotherapy

Abstract

Introduction: The purpose of this study is to describe variations in microvasculature before and after treatment of treatment-naive lesions and during consolidation therapy of retinoblastoma lesions using an investigational portable optical coherence tomography angiography (OCTA) system. ***Methods:*** This study is a single-center, prospective, observational case series. Recruited subjects were either undergoing surveillance for retinoblastoma or had newly detected retinoblastoma. Nine tumors from 7 eyes in 6 patients were included. During exams under anesthesia, the tumors were imaged with an investigational portable OCTA system. OCTA images were analyzed to assess vascular changes before and after treatment. ***Results:*** In all 6 presented cases, OCTA imaging revealed distinctive vascular patterns, such as dilated feeder arteries and draining veins, disorganized and complex branching patterns, irregular vessel calibers, and dilation and tortuosity of vessels. After treatment, OCTA imaging revealed decreased intrinsic tumor vascularity and reduced dilation of draining and feeder vessels. Tumor relapse demonstrated prominent vascularity ($n = 1$) that resolved on repeat OCTA after transpupillary thermotherapy treatment. Type 2 ($n = 1$), 3 ($n = 6$), and 4 ($n = 1$) tumor regression patterns were seen in our patients after treatment, and OCTA findings were consistent with a previously published report. Interestingly, in one of the presented cases, OCTA demonstrated clear feeder, draining, and intrinsic tumor vessels that were not as evident on fluorescein angiography. ***Conclusions:*** OCTA may offer a noninvasive and sensitive technique to evaluate the vasculature of both the tumor and the surrounding retina in retinoblastoma. With additional research and development into its use in patients with retinoblastoma, OCTA may one day be useful in assessing treatment response and residual tumor activity.

© 2021 S. Karger AG, Basel

Introduction

Retinoblastoma is the most common primary malignant intraocular tumor in childhood [1]. Retinoblastoma tumors on ophthalmoscopy can present as elevated white or translucent retinal masses of different sizes, with lesions that can show intralesional calcifications and dilated feeder and draining blood vessels [1]. Over the last 10 years, there has been a significant evolution in treatment options for retinoblastoma [2]. The various avail-

karger@karger.com
www.karger.com/oop

© 2021 S. Karger AG, Basel

Correspondence to:
Miguel Angel Materin, miguel.materin@duke.edu

Karger

Table 1. Summary of treatment history and type of regression pattern of imaged retinoblastoma lesions

Case	Eye	Tumor no.	Prior treatment	Clinical regression pattern
1	OD	1	None	None
2	OS	1	Systemic chemotherapy (2 cycles) and TTT (2 sessions)	3
	OS	2	Systemic chemotherapy (2 cycles) and TTT (2 sessions)	3
3	OS	1	Systemic chemotherapy (6 cycles), IAC (2 rounds), TTT (5 sessions), and TTT (2 sessions over relapse area)	3
4	OD	1	Systemic chemotherapy (3 cycles) and TTT (1 session)	2
	OD	2	Systemic chemotherapy (3 cycles) and TTT (1 session)	4
	OS	1	Systemic chemotherapy (3 cycles) and TTT (1 session)	3
5	OS	1	IAC (3 rounds) and TTT (4 sessions)	3
6	OS	1	IAC (2 rounds) and TTT (3 sessions)	3

Systemic chemotherapy: vincristine, etoposide, and carboplatin. TTT, transpupillary thermotherapy; IAC, intra-arterial chemotherapy (melphalan).

able treatments now include the use of multiple agent systemic chemotherapy, intra-arterial chemotherapy (IAC), intravitreal chemotherapy, brachytherapy, transpupillary thermotherapy (TTT), and cryotherapy, among others [2]. A combination of these therapeutic tools can be used depending on the clinical characteristics of the tumors, treatment preferences of the treating specialist, and availability of treatment modalities [2]. This wealth of treatment options has allowed retinoblastoma to become the most curable cancer in children in developed nations [2].

Ancillary tests such as handheld spectral-domain OCT and fluorescein angiography (FA) images can be utilized in the evaluation and monitoring of retinoblastoma patients. There are several reports in the literature describing the appearance of active retinoblastoma tumors, preretinal seeds, and the characteristic findings of early small lesions using these imaging modalities [1, 3, 4]. On FA, retinoblastoma tumors may demonstrate large and small retinal vessel abnormalities and intrinsic tumor vessels [5]; serial FA images can be used to monitor vascular changes after treatment and, in some cases, identify early recurrences [6–8]. However, FA is invasive and largely relies on the IV injection of fluorescein dye.

Optical coherence tomography angiography (OCTA) is a relatively new imaging technique that allows visualization of retinal and choroidal vascular patterns without many of the disadvantages that occur with FA [9–15]. Additionally, and importantly, OCTA allows for depth-encoded visualization of vascular networks through the different depths of the retina. The development of an investigational handheld OCTA device has made imaging in the operating room a possibility over the last few years. Distinct vascular patterns associated with different types of retinoblastoma lesion regression patterns have previously been reported, and here, we further demonstrate increased vascular density and the presence of dilated feeder vessels on OCTA of active lesions [15]. To the best of our knowledge, this is the first report to evaluate vascular changes before and after treatment of retinoblastoma tumors on OCTA and to corroborate the previously mentioned OCTA findings with different tumor regression patterns.

Materials and Methods

With approval of the Duke Institutional Review Board, children undergoing surveillance for retinoblastoma or with newly detected retinoblastoma were recruited after obtaining written parental consent. This exploratory study adhered to the tenets of the Declaration of Helsinki and the Health Insurance Portability and Accountability Act. Recruited subjects were those with a known or suspected diagnosis of retinoblastoma who were undergoing a planned examination under anesthesia (EUA). Both treatment-naive patients and patients who had undergone treatment were included. All EUAs and local treatments were performed by the same physician (M.A.M.). Eyes were graded using the International Classification of Retinoblastoma. During the EUA, the tumors were imaged with an investigational portable OCTA system (Spectralis with Flex and OCTA module; Heidelberg Engineering, Heidelberg, Germany), and imaging was performed as previously described [11]. Automated and manual segmentation of the retinal layers was difficult or not possible in tumor areas due to disorganization and obliteration of normal cellular boundaries.

Table 2. Comparison of retinoblastoma lesions imaged with OCTA before and after TTT

Case	Eye	Tumor no.	Intrinsic tumor vascularity	Dilation of draining and feeder vessels
1	OD	1	Decreased	Reduced
2	OS	1	Decreased	Reduced
	OS	2	No change	No change
3	OS	1	Decreased	Reduced

OCTA, optical coherence tomography angiography; TTT, transpupillary thermotherapy.

Results

A summary of treatment history and type of regression pattern of the imaged retinoblastoma lesions is summarized in Table 1. Changes in vascular characteristics before and after TTT treatment are summarized in Table 2.

Case 1 was a treatment-naive 2-month-old male who presented with unilateral retinoblastoma and subsequently underwent TTT treatment. OCTA imaging was acquired before, immediately after, and at 1-month post-treatment. FA was acquired pretreatment. On ophthalmoscopy, there was a translucent retinal lesion in the right eye inferonasal to the optic nerve, consistent with group A retinoblastoma (Fig. 1a).

Before any treatment was done, the FA of the right eye demonstrated slight hyperfluorescence over the lesion (Fig. 1b). The OCT B-scan over the lesion with flow overlay showed a hyperdense intraretinal smooth lesion with distinct borders centered in the inner nuclear layer involving the middle retinal layers (Fig. 1c). OCTA showed a circumferential network of dilated feeder and draining vessels and a dense vascular network of intrinsic vessels, at various depths on cross-sectional OCTA images (Fig. 1d).

Fundus photography of the right eye immediately after TTT revealed a white area corresponding to the treated lesion (Fig. 1e). OCT B-scan showed increased hyper-reflectivity over a larger hyperdense area with less distinct margins compared to lesion before treatment (Fig. 1f). OCTA revealed no significant difference in the vascular pattern of the lesion, with slightly fewer intrinsic vessels at the center of the tumor (Fig. 1g).

At 1-month post-TTT, atrophy and fibrosis consistent with scar formation were noted overlying the previously treated lesion (Fig. 1h). OCT B-scan over the lesion with flow overlay still demonstrated a more atrophic appearance to the retinoblastoma lesion with a decrease in flow (Fig. 1i). OCTA showed a corresponding decrease in intrinsic vascularity overlying the lesion (Fig. 1j). The draining and medium-sized feeder vessels appeared less dilated, and there appeared to be areas of traction around adjacent vessels (Fig. 1j).

Fundus photograph of the right eye immediately after a second round of TTT showed a white lesion with overlying retinal hemorrhages (Fig. 1k). OCT B-scan over the lesion with flow overlay showed an increase in lesion reflectivity (Fig. 1l). OCTA showed further reduced intrinsic vessels, and the lesion appeared mildly hyper-reflective, still causing traction of the surrounding vessels (Fig. 1m).

Case 2 was a 2-year-old male with bilateral retinoblastoma, group E retinoblastoma in the right eye and group C retinoblastoma in the left eye. He was undergoing systemic chemotherapy with 2 completed cycles. The right eye was treated with enucleation, and the left eye had 2 lesions that were both treated with TTT (Fig. 2a). OCTA images were acquired before, immediately after, and 1 month after the patient's third session of TTT treatment to both lesions.

On ophthalmoscopy, both lesions in the left eye demonstrated a type 3 regression pattern (partially calcified remnant) before (Fig. 2a) and immediately after (Fig. 2f) TTT. Before the third TTT session, the OCT B-scan over lesion 1 with flow overlay showed a cystic superficial area in the superior layers of the lesion and a hyperdense intraretinal lesion in the deeper layers that affected the remaining retinal layers (Fig. 2d). The OCT B-scan over lesion 2 with flow overlay depicts an elevated hyperdense area involving all retinal layers (Fig. 2e). OCTA over lesion 1 showed a superficial circumferential network of disorganized dilated medium-sized vessels surrounding the cystic area, and this area showed a small intrinsic vascular network at a deeper aspect of the lesion (Fig. 2b). OCTA over lesion 2 showed large dilated vessels creating a dense intrinsic vascular network of tortuous medium-sized dilated vessels in the lesion (Fig. 2c). OCTA images of both lesions immediately after the third TTT did not show significant changes compared to pre-TTT, besides a slight decrease in intrinsic vascularity at a deeper level of lesion 1 cystic area (Fig. 2g, h).

Fundus photograph of the left eye 1-month post-TTT revealed a decrease in size of both lesions (Fig. 2i). OCTA of lesion 1 showed decreased deeper intrinsic vascularity and a modest reduction in the dilation of the medium-sized vessels (Fig. 2j). OCTA of lesion 2 did not show significant changes (Fig. 2k).

Case 3 was a 2-year-old male with bilateral retinoblastoma, group A retinoblastoma type 4 regression pattern

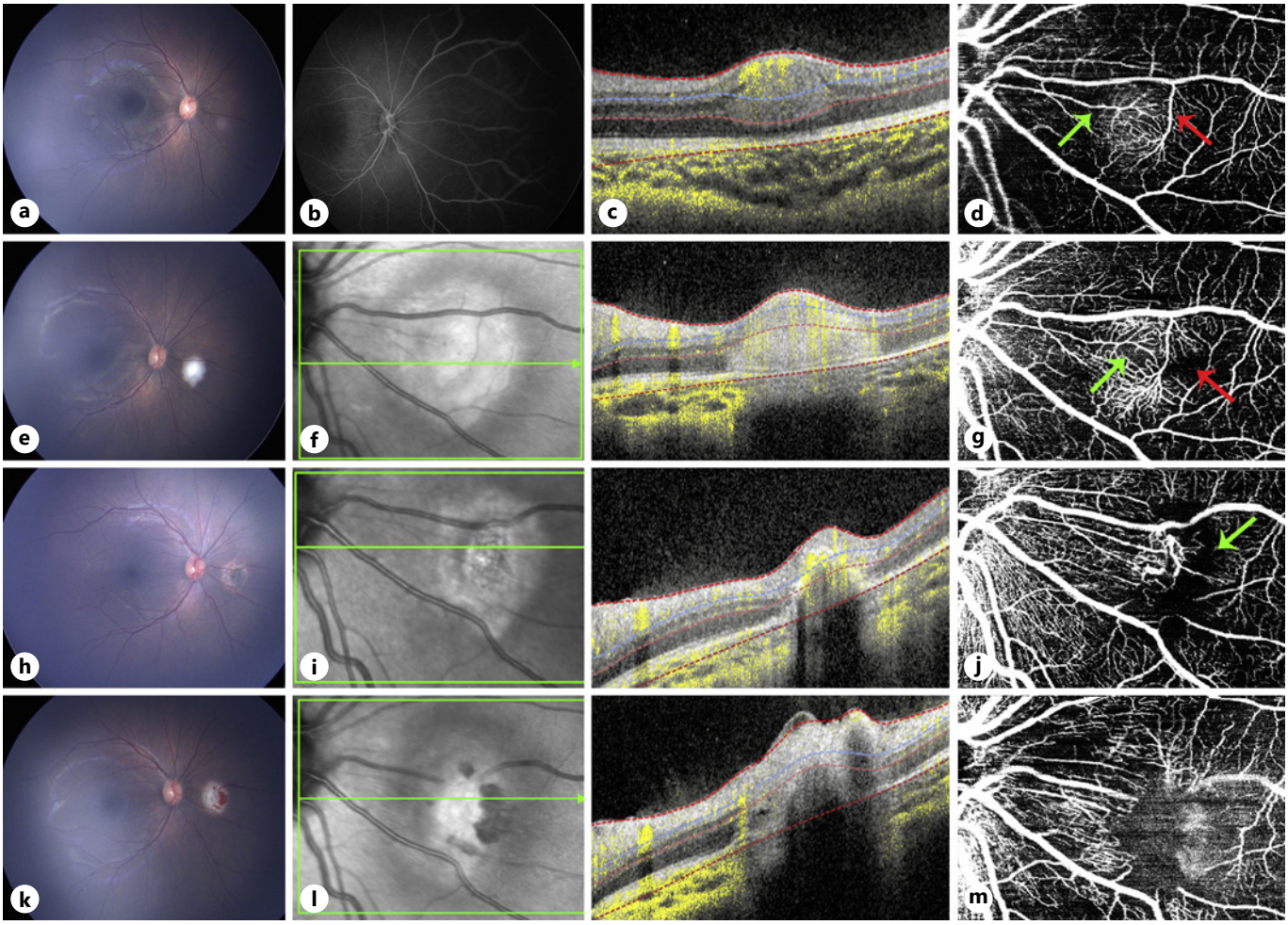

Fig. 1. Multimodal image of case 1. **a** Color fundus photograph of a treatment-naive retinoblastoma lesion in the right eye. **b** FA only revealed mild hyperfluorescence at lesion area. **c** OCT B-scan showing a well-circumscribed hyper-reflective lesion involving retinal mid-layers. **d** En face 20 × 20° OCTA revealed the feeder and draining dilated vessels (green arrow and red arrow, respectively) and dense intrinsic vascularity. **e** Color fundus photograph of the same eye immediately after the first TTT. **f** OCT B-scan of the same lesion immediately after the first TTT shows an enlargement, not definite margins, and an increase in hyper-reflectivity compared to pre-TTT. **g** En face 20 × 20° OCTA immediately after first TTT does not show major vascular differences apart from an increase in vessel reflectivity and less perfused areas (green and red arrows). **h** Color fundus photograph 1 month after the first TTT of the same tumor. **i** OCT B-scan shows shrinkage of the lesion with indistinct borders. **j** En face 20 × 20° OCTA 1 month after the first TTT treatment revealed a drastic decrease in intrinsic vessel network density replaced with a dark area (green arrow), with retraction of the draining and feeder vessels and traction of surrounding vessels from the treated lesion. **k**–**m** correspond to images immediately after second TTT, showing a similar effect obtained immediately after the first TTT treatment was done. **m** En face 20 × 20° OCTA obtained immediately after the second TTT revealed minimum tumor intrinsic vascular network replaced by a dark mild hyper-reflective area due to inflammation caused by treatment. FA, fluorescein angiography; OCTA, optical coherence tomography angiography; TTT, transpupillary thermotherapy.

(flat scar) in the right eye and group B retinoblastoma with a type 3 regression pattern in the left eye. He was treated with 6 cycles of systemic chemotherapy. Both eyes were previously treated with TTT, and the left eye had previously undergone 2 sessions of IAC. The left eye was noted to have a tumor relapse along the inferior portion of the lesion (Fig. 3a). OCTA imaging was acquired before the third TTT treatment over tumor relapse area and immediately post-TTT treatment.

On ophthalmoscopy of the left eye before the third TTT, there was a lesion located in the posterior pole with the superior portion showing calcification and fibrosis

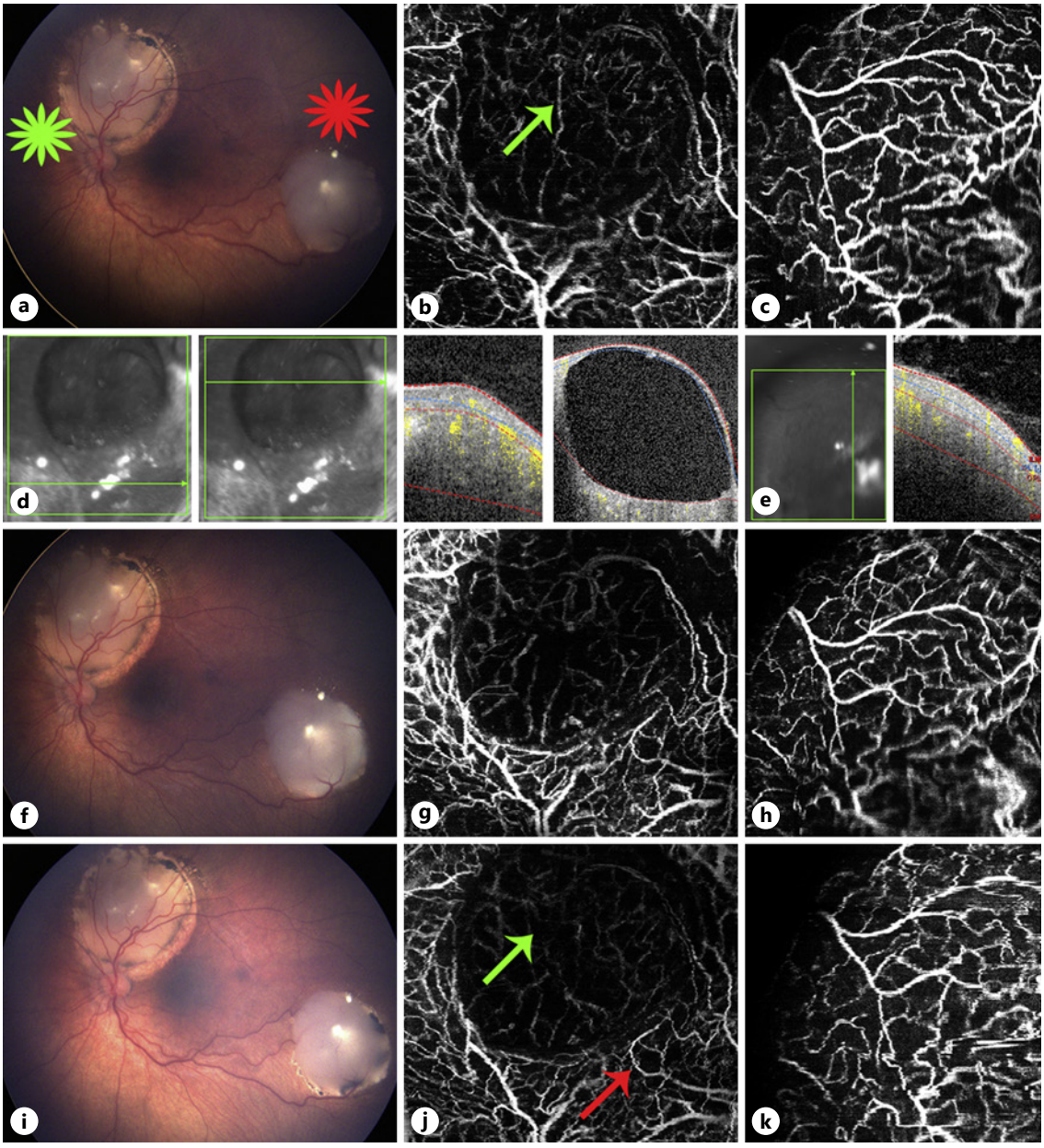

Fig. 2. Multimodal image of case 2. **a** Color fundus photograph of retinoblastoma lesion 1 (green star) and lesion 2 (red star), both with type 3 regression in the left eye. **b** En face 20 × 20° OCTA of lesion 1 shows a circumferential network of mid-size dilated vessels around a cystic area, which shows intrinsic vascularity at a deeper level. **c** En face 20 × 20° OCTA of lesion 2 shows large dilated vessels forming a dense intrinsic vascular network of tortuous medium-sized dilated vessels. **d** OCT B-scans over lesion 1 shows a non-cystic area of the lesion with a hyper-reflective lesion involving all retinal layers and another cut over the cystic area, which also shows a solid vascularized area deeper to the cyst. **e** OCT B-scan over lesion 2 shows an elevated hyperdense lesion involving all retinal layers. **f** Color fundus photograph immediately taken after the third TTT. En face 20 × 20° OCTA over lesion 1 did not show any major changes compared to image before treatment, apart from a slight decrease in the intrinsic vascularity deeper to the cystic area (**g**), and OCTA over lesion 2 did not show any changes (**h**). **i** Color fundus photograph of retinoblastoma lesion 1 and lesion 2 at 1 month after the third TTT shows shrinkage of both lesions specially noted at their borders. **j** En face 20 × 20° OCTA of lesion 1 1 month after TTT shows a decrease in intrinsic vascularity at a deeper level of the lesion under the cystic area (green arrow) and a reduction in the dilation of the medium-sized vessels surrounding the cystic portion (red arrow). **k** OCTA of lesion 2 did not express any changes. OCTA, optical coherence tomography angiography; TTT, transpupillary thermotherapy.

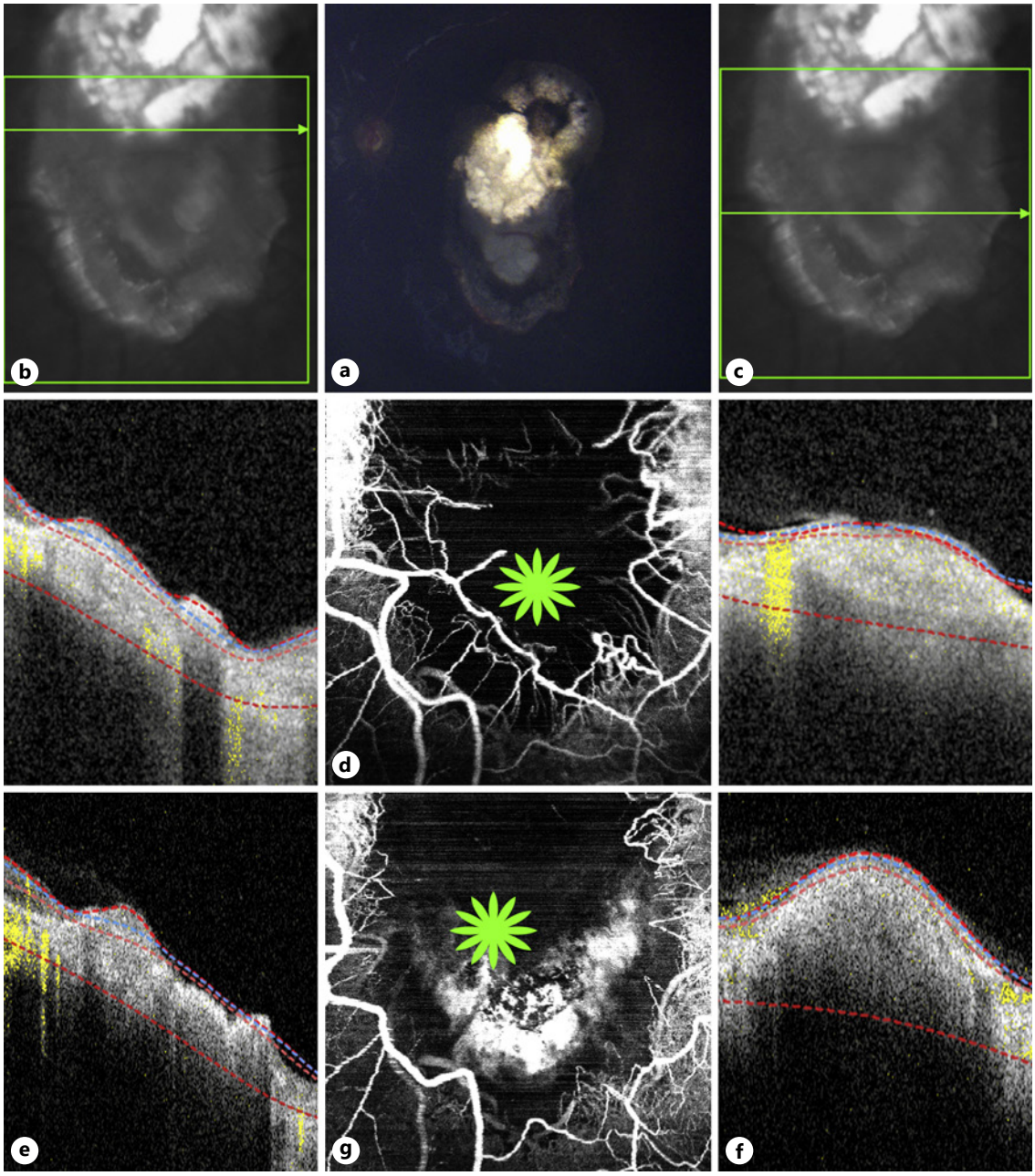

Fig. 3. Multimodal image of case 3. **a** Color fundus photograph of a retinoblastoma lesion with type 3 regression and a tumor recurrence at the inferior aspect of the lesion in the left eye. OCT B-scans (**b**) over the superior portion showing a disorganized retinal atrophic area and another cut (**c**) over the tumor relapse depicting an elevated hyper-reflective lesion. **d** En face 20 × 20° OCTA shows a network of dilated tortuous medium-sized vessels at the borders of tumor relapse and a dark area at the center revealing absence of vessels. OCT B-scans over the same areas immediately after the third TTT session with the superior portion (**e**) still having an atrophic appearance and over the relapse area (**f**), an increase in size and reflectivity compared to pre-TTT (**c**) due to tissue inflammation caused by the treatment. **g** En face 20 × 20° OCTA over the same area immediately after the third TTT shows the dilated vessels surrounding the relapse are not present and next to that area a hyper-reflective signal (green star) caused by the treatment inflammation. OCTA, optical coherence tomography angiography; TTT, transpupillary thermotherapy.

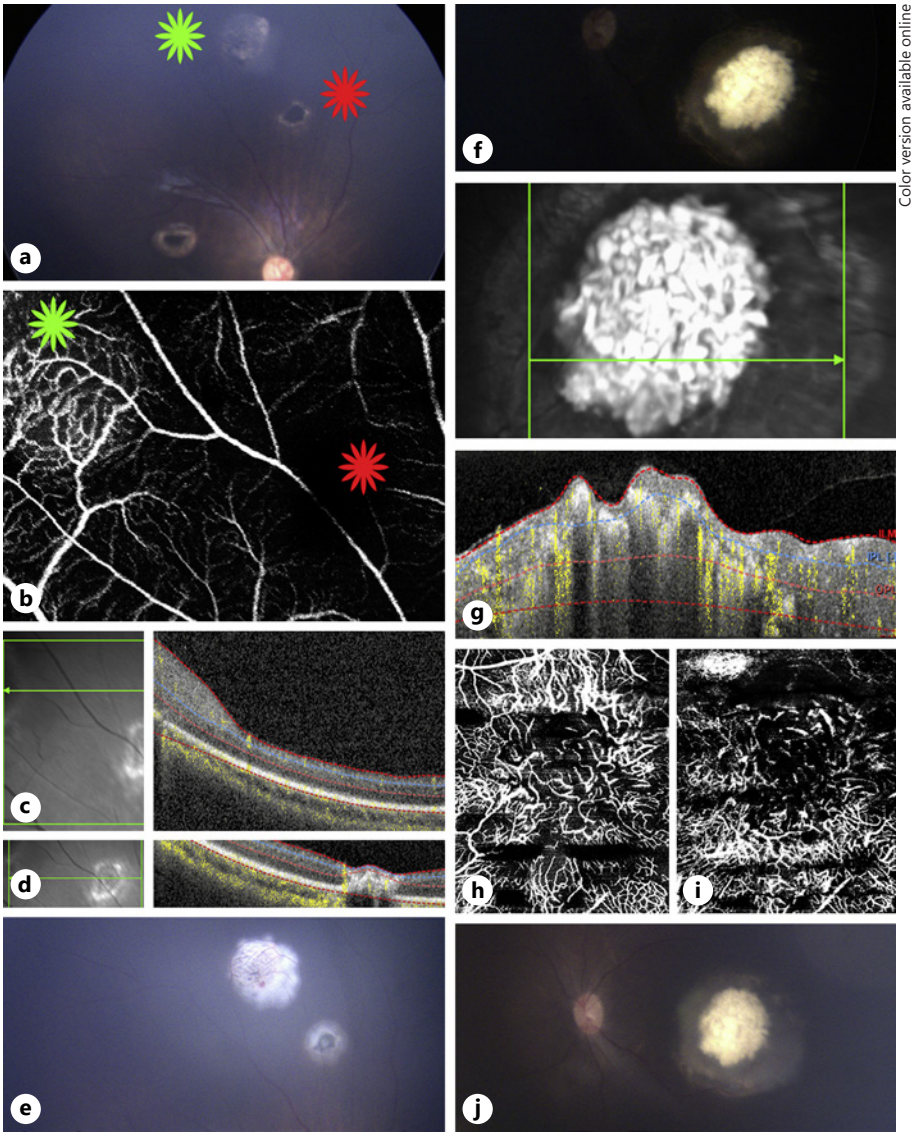

Fig. 4. Multimodal image of case 4. **a** Color fundus photograph of retinoblastoma lesion 1 with type 2 regression (green star) and lesion 2 with type 4 regression (red star) of the right eye 1 month after the first TTT. **b** En face 20 × 20° OCTA shows that lesion 1 with a type 2 regression pattern has dilated feeder and draining vessels around a dense network of intrinsic vessels (green star) compared to the signal void area at the location of lesion 2 (red star), which has a type 4 regression pattern. OCT B-scans over lesion 1 (**c**) and lesion 2 (**d**) show an elevated hyper-reflective lesion and an atrophic area, respectively. **e** Color fundus photograph of the same lesions immediately after the second TTT. **f** Color fundus photograph of a retinoblastoma lesion with a type 3 regression pattern but mostly calcified very close to turning into a type 1 regression pattern in the left eye 1 month after the first TTT. **g** OCT B-scan shows an elevated lesion with an irregular anterior border and intralesional calcifications generating shadowing. En face 20 × 20° OCTA of the left eye shows on the superficial portion of the lesion a dense intrinsic vascular network formed by fine vessels (**h**) and OCTA at the deeper part of the tumor depicts various dark areas caused by shadowing from calcifications and a more tortuous network of vessels (**i**). **j** Color fundus photograph of the left eye lesion immediately after the second TTT session. OCTA, optical coherence tomography angiography; TTT, transpupillary thermotherapy.

and a newly detected elevation on the inferior portion representing a tumor relapse (Fig. 3a). The OCT B-scan over the lesion with flow overlay showed an atrophic retina at the superior aspect of the lesion and an elevated hyperdense retinal lesion at the tumor relapse (Fig. 3b, c, respectively) with an increase in lesion thickness seen after TTT (Fig. 3e, f). Pretreatment OCTA showed a circumferential network of dilated medium-sized vessels at the borders of tumor relapse and non-perfusion areas at the center of the imaged lesion area (Fig. 3d). OCTA images immediately acquired post-TTT showed a hyper-reflective area inferiorly and the absence of many dilated medium-sized vessels that were located at borders of tumor relapse (Fig. 3g).

Case 4 was a 4-month-old male with bilateral group B retinoblastoma. The patient was undergoing systemic chemotherapy with 3 completed cycles. The lesions in both eyes were previously treated with TTT. OCTA imaging was acquired 1 month after the first session of TTT to lesions in both eyes. Of the lesions in the right eye, the superior (lesion 1) had a type 2 regression pattern (non-calcified remnant) and another lesion (lesion 2) that was more inferior had a type 4 regression pattern (flat scar) (Fig. 4a). OCT B-scan over the lesion with flow overlay showed an elevated hyperdense retinal lesion involving all the retinal layers (lesion 1) (Fig. 4c) and a mostly atrophic retinal lesion (lesion 2) (Fig. 4d). OCTA showed a circumferential network of dilated medium-sized feeder

Ocul Oncol Pathol 2021;7:330–339
DOI: 10.1159/000515142

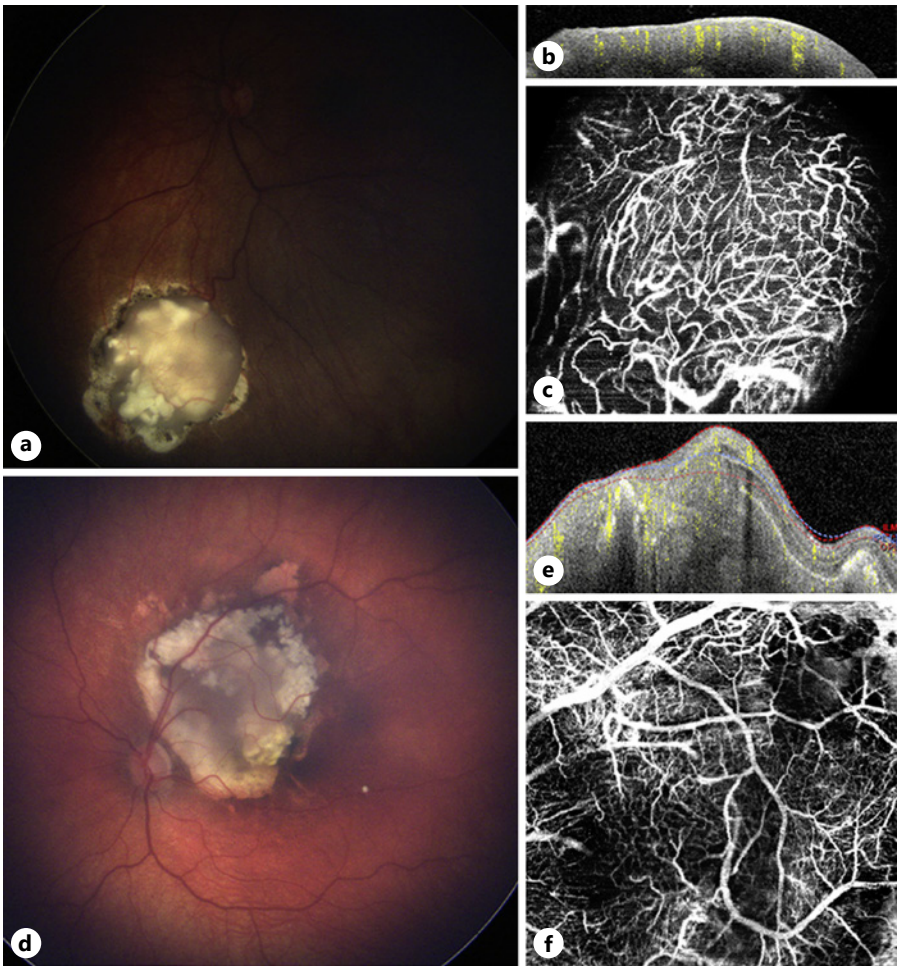

Fig. 5. Multimodal image of cases 5 and 6. **a** Color fundus photograph of a retinoblastoma lesion from case 5 with type 3 regression in the left eye, 1 month after the fourth TTT session. **b** OCT B-scan over the tumor shows an elevated vascularized hyper-reflective lesion involving all retinal layers. **c** En face 20 × 20° OCTA of the lesion shows a network of tortuous and dilated medium- and small-sized vessels. **d** Color fundus photograph of a retinoblastoma lesion from case 6 with type 3 regression with a cystic area at the temporal superior border in the left eye, 1 month after the third TTT session. **e** OCT B-scan over the lesion showing an elevated hyper-reflective lesion with an irregular anterior border and intralesional calcifications causing shadowing. **f** En face 20 × 20° OCTA of the same lesion shows a disorganized network of tortuous dilated and large-, medium-, and small-sized vessels and a dark area at the superotemporal border caused by the cystic portion and intralesional calcifications. OCTA, optical coherence tomography angiography; TTT, transpupillary thermotherapy.

and draining vessels and a dense vascular network of small intrinsic vessels (at various depths on cross-sectional OCTA images) of lesion 1 and no vascularity over lesion 2 (Fig. 4b).

Fundus photograph of the left eye revealed a tumor at the posterior pole with a type 3 regression pattern but was mostly calcified (Fig. 4f). OCT B-scan over the lesion with flow overlay revealed an elevated irregular retinal tumor with hyperdense areas within the lesion causing shadowing compatible with calcifications (Fig. 4g). OCTA through the superficial aspect of the lesion showed a dense intrinsic vascular network with fine vessel caliber (Fig. 4h), whereas OCTA through a deeper aspect of the lesion showed a more tortuous network of intrinsic vessels and shadowing from the calcifications (Fig. 4i). Another session of TTT was performed for all lesions described in both eyes (Fig. 4e, j).

Case 5 was a 3-year-old male with unilateral group B retinoblastoma with type 3 regression pattern in the left eye. The patient had previously received 3 rounds of IAC. The left eye was treated with TTT, and OCTA imaging was acquired 1 month after the fourth TTT session. On ophthalmoscopic exam of the left eye, there was a partially calcified retinal lesion located in the inferonasal quadrant (Fig. 5a). The OCT B-scan over the lesion with flow overlay showed a vascularized highly elevated hyperdense retinal lesion (Fig. 5b). The OCTA revealed a disorganized network of dilated medium- and small-sized tortuous vessels within the imaged lesion (Fig. 5c). This lesion also underwent a fifth session of TTT.

Case 6 was a 15-month-old male with unilateral retinoblastoma, group C retinoblastoma with type 3 regression pattern in the left eye. The patient had previously received 2 rounds of IAC. The left eye was treated with TTT, and OCTA imaging was acquired 1 month after the third TTT session. On ophthalmoscopic exam of the left eye, there was a posterior pole lesion located temporal to the optic nerve (Fig. 5d). OCT B-scan with flow overlay

over the lesion showed a vascularized elevated hyperdense retinal lesion with areas of shadowing due to intralesional calcifications (Fig. 5e). OCTA showed an erratic network of dilated large-, medium-, and small-sized tortuous vessels and a dark border at the temporal side of the imaged lesion area due to shadowing caused by a cystic area and calcifications (Fig. 5f). A fourth TTT session was done to the described lesion.

Discussion and Conclusions

To the best of our knowledge, this case series is the first descriptive analysis comparing pre- and posttreatment OCTA images of retinoblastoma lesions. The presented cases confirmed previously reported vascular patterns related to each type of regression pattern and how the vascular patterns seen on OCTA relate to disease activity [15].

The first 2 cases highlight the vascular changes that can be seen on OCTA 1 month after TTT treatment. Both cases demonstrated decreased intrinsic tumor vascularity and reduced dilation of draining and feeder vessels, especially seen in case 1, in which some areas of the intrinsic tumor vascularity were completely replaced with dark areas, representing zones of no vascular flow. These vascular changes have been reported on FA by other authors [6–8]. These findings also correlate with OCT B-scans, as shown in case 1, where the initially elevated hyperdense intraretinal lesion with distinct borders transforms into a not well-limited lesion with atrophic appearance at 1 month from the first TTT session, as has previously been reported [1, 3, 4].

Post-inflammatory changes are noted on ophthalmoscopy immediately after TTT treatment in the first 3 cases. On OCT B-scans over the active tumors, these tumors appear as smooth hyperdense intraretinal lesions with distinct borders that increase in size and reflectivity with less distinct margins after TTT. These alterations on OCT B-scans likely represent an inflammatory response from the TTT treatment. On OCTA images, the vascularity appears to decrease slightly after TTT. It is possible that this may represent an artifact from the resultant inflammation versus a true decrease in vascularity.

Retinoblastoma relapse was seen in case 3. Tumor relapses have previously been described on FA as having prominent vessels stemming from a scar adjacent to the tumor relapse [6]. OCTA obtained prior to TTT demonstrated prominent vascularity that was no longer evident on repeat OCTA imaging immediately following TTT treatment. This may represent a decrease in vascularity or blockage caused by treatment-induced inflammation.

In all 6 presented cases, OCTA demonstrated vascular patterns that were consistent with previously published reports on retinoblastoma lesions imaged with FA [5–8]. These patterns include dilated feeder arteries and draining veins, disorganized and complex branching patterns, irregular vessel calibers, dilation, and tortuosity [5–8]. Additionally, the presented cases demonstrated vascular patterns associated with the different types of retinoblastoma tumor regression, as previously reported by Thomas et al. [15], and our findings adhere to their hypothesis that lesions with more intense vascular density and dilated feeder/draining vessels on OCTA images are persistently active, compared to inactive lesions. These findings on OCTA include a retinoblastoma lesion with type 1 regression with the superficial aspect of the lesion showing a dense intrinsic vascular network with fine vessel caliber and a more tortuous network of intrinsic vessels at a deeper aspect of the lesion with shadowing from calcifications. Retinoblastoma lesions with type 2 regression patterns showed prominent feeder vessels and dense intrinsic vascularity. The most frequent regression pattern seen in lesions of our case series was the type 3 regression, which showed a combination of what was found on OCTA images of both type 1 and type 2 regression patterns. Finally, tumors having a type 4 regression pattern show a dark area on OCTA, proving no active flow.

It is also important to mention that, as reflected in our first case, OCTA revealed feeder, draining, and intrinsic vessels that were not detected on FA. This was a surprising finding since most vascular changes are detected on FA but may represent how OCTA may be more sensitive at detecting very immature vessels associated with new lesions. More investigation is needed to confirm this finding, but as OCTA technology advances and is made more available, more reports may surface to correlate this finding.

These cases demonstrate that OCTA images could be useful to evaluate residual intrinsic vascularity and feeder vessel dilation in response to treatment and to monitor for tumor relapses. As previously reported, higher tumor vessel densities may be associated with greater risk for local invasive growth [16] and residual intrinsic vascularity may represent active disease [7]. FA can be utilized to evaluate these vascular changes, but our cases illustrate that OCTA may offer a noninvasive and sensitive technique to evaluate intrinsic tumor and surrounding retinal vasculature.

Limitations of this study include a small number of imaged patients and technical difficulties in obtaining reli-

able images. Frequent corneal surface lubrication helped improve image quality. OCTA images could not be acquired for all the patients at 1 month due to an institutional requirement to halt all nonessential clinical activity during the COVID-19 pandemic. A second limitation is related to the segmentation of the standard layers. The standard retinal layers with their corresponding vascular complexes could not be obtained due to lesions altering the retinal normal architecture. Manual segmentation was performed for OCTA image analysis, with thick lesions requiring more manual correction. Image artifacts such as shadowing from calcifications obscured the view of some of the deeper vessels. Additional limitations related to OCTA imaging include a limited field of view, not being able to image peripheral lesions, and the difficulty of capturing the complete area of large lesions in the same image.

OCTA imaging of retinoblastoma lesions before and after different treatment modalities could be useful in assessing treatment response and residual tumor activity. Standard protocols for retinoblastoma OCTA images and interpretation are needed to be done based on a larger sample of patients with early and late follow-up.

Statement of Ethics

With approval of the Duke Institutional Review Board (IRB: Pro00065236), children with newly detected retinoblastoma or undergoing surveillance for retinoblastoma were recruited after obtaining written parental consent. This exploratory study adhered to the tenets of the Declaration of Helsinki and the Health Insurance Portability and Accountability Act.

Conflict of Interest Statement

M.A.M. is a consultant to Castle Biosciences and Astra Zeneca. L.V. receives support from the Heidelberg Engineering through the Heidelberg Engineering Grant, which includes use of research equipment. The following authors have no financial disclosures: J.P.F., A.A.H., A.P., and M.P.K.

Funding Sources

No funding or grant support.

Author Contributions

All authors contributed to this study and attest that they meet the current ICMJE criteria for authorship.

References

1 Liu KC, Walter SD, Finn AP, Materin MA. Venous loop reveals an occult retinoblastoma tumor. Ophthalmic Surg Lasers Imaging Retina. 2017;48(9):768–70.
2 Abramson DH, Shields CL, Munier FL, Chantada GL. Treatment of retinoblastoma in 2015: agreement and disagreement. JAMA Ophthalmol. 2015;133(11):1341–7.
3 Rootman DB, Gonzalez E, Mallipatna A, VandenHoven C, Hampton L, Dimaras H, et al. Hand-held high-resolution spectral domain optical coherence tomography in retinoblastoma: clinical and morphologic considerations. Br J Ophthalmol. 2013;97(1):59–65.
4 Finn AP, House RJ, Hsu ST, Thomas AS, El-Dairi MA, Freedman S, et al. Hyperreflective vitreous opacities on optical coherence tomography in a patient with bilateral retinoblastoma. Ophthalmic Surg Lasers Imaging Retina. 2019;50(1):50–2.
5 Kim JW, Ngai LK, Sadda S, Murakami Y, Lee DK, Murphree AL. Retcam fluorescein angiography findings in eyes with advanced retinoblastoma. Br J Ophthalmol. 2014;98(12):1666–71.
6 Ohnishi Y, Yamana Y, Minei M, Ibayashi H. Application of fluorescein angiography in retinoblastoma. Am J Ophthalmol. 1982;93(5):578–88.
7 Shields JA, Sanborn GE, Augsburger JJ, Orlock D, Donoso LA. Fluorescein angiography of retinoblastoma. Retina. 1982;2(4):206.
8 Bianciotto C, Shields CL, Iturralde JC, Sarici A, Jabbour P, Shields JA. Fluorescein angiographic findings after intra-arterial chemotherapy for retinoblastoma. Ophthalmology. 2012;119(4):843–9.
9 Chen X, Viehland C, Carrasco-Zevallos OM, Keller B, Vajzovic L, Izatt JA, et al. Microscope-integrated optical coherence tomography angiography in the operating room in young children with retinal vascular disease. JAMA Ophthalmol. 2017;135(5):483–6.
10 House RJ, Hsu ST, Thomas AS, Finn AP, Toth CA, Materin MA, et al. Vascular findings in a small retinoblastoma tumor using OCT angiography. Ophthalmol Retina. 2019;3(2):194–5.
11 Hsu ST, Chen X, Ngo HT, House RJ, Kelly MP, Enyedi LB, et al. Imaging infant retinal vasculature with OCT angiography. Ophthalmol Retina. 2019;3(1):95.
12 Hsu ST, Ngo HT, Stinnett SS, Cheung NL, House RJ, Kelly MP, et al. Assessment of macular microvasculature in healthy eyes of infants and children using OCT angiography. Ophthalmology. 2019;126(12):1703–11.
13 Nadiarnykh O, Davidoiu V, Gräfe MGO, Bosscha M, Moll AC, De Boer JF. Phase-based OCT angiography in diagnostic imaging of pediatric retinoblastoma patients: abnormal blood vessels in post-treatment regression patterns. Biomed Opt Express. 2019;10(5):2213–26.
14 Sioufi K, Say EAT, Ferenczy SC, Leahey AM, Shields CL. Optical coherence tomography angiography findings of deep capillary plexus microischemia after intravenous chemotherapy for retinoblastoma. Retina. 2019;39(2):371–8.
15 Thomas AS, Hsu ST, House RJ, Finn AP, Kelly MP, Toth CA, et al. Microvascular features of treated retinoblastoma tumors in children assessed using OCTA. Ophthalmic Surg Lasers Imaging Retina. 2020;51(1):43–9.
16 Rössler J, Dietrich T, Pavlakovic H, Schweigerer L, Havers W, Schüler A, et al. Higher vessel densities in retinoblastoma with local invasive growth and metastasis. Am J Pathol. 2004;164(2):391–4.